

TCAD simulation I

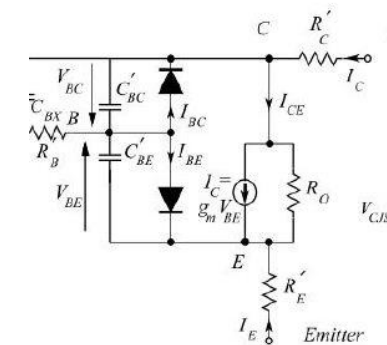
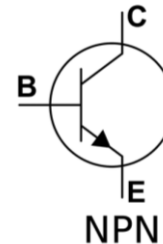
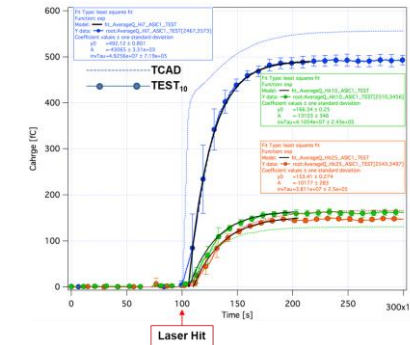
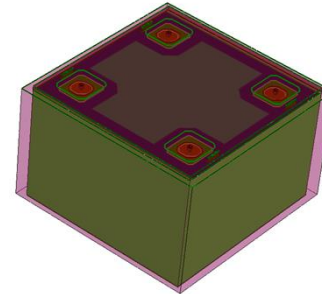
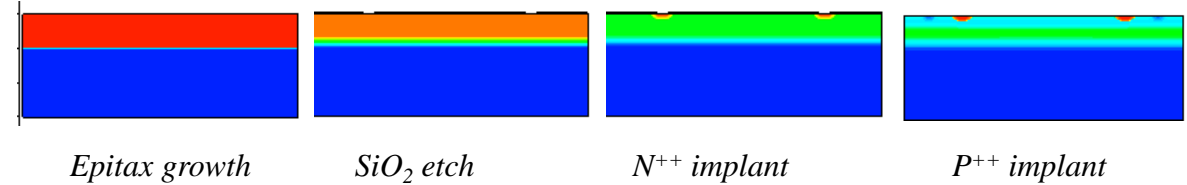
E. Giulio Villani

Overview

- **Introduction, needs for TCAD simulations**
- **Transport regimes and related equations**
- **Discretization techniques: meshing**
- **Discretization of semiconductor equations: Scharfetter-Gummel technique**
- **Examples**

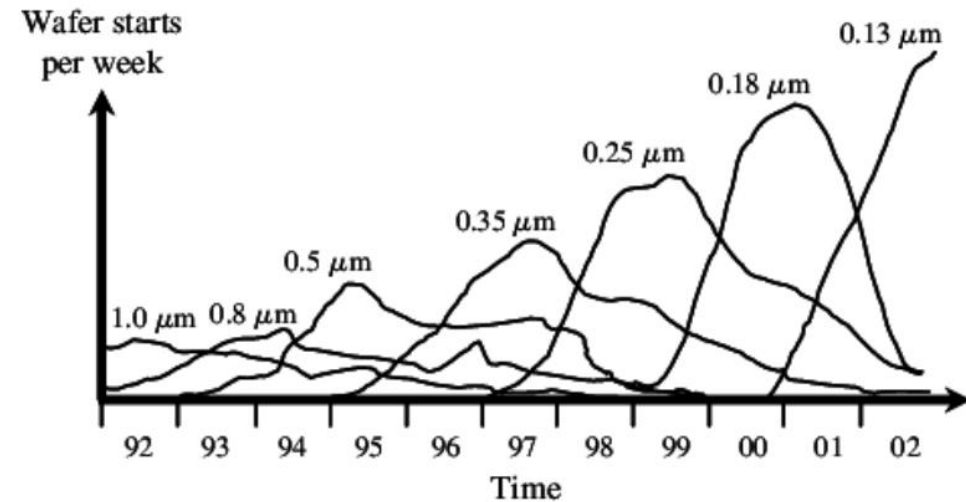
Introduction

- TCAD (Technology Computer Aided Design) divides into three groups:
 - **Process simulation**, i.e. simulation of fabrication process steps (oxidation, implantation, diffusion...)
 - **Device simulation**, i.e. simulation of the thermal/electrical/optical behavior of electronic devices, (IV, CV, frequency response...)
 - **Device modeling**, i.e. creating compact behavioral models for devices for circuit simulation (SPICE, Cadence...)



Introduction

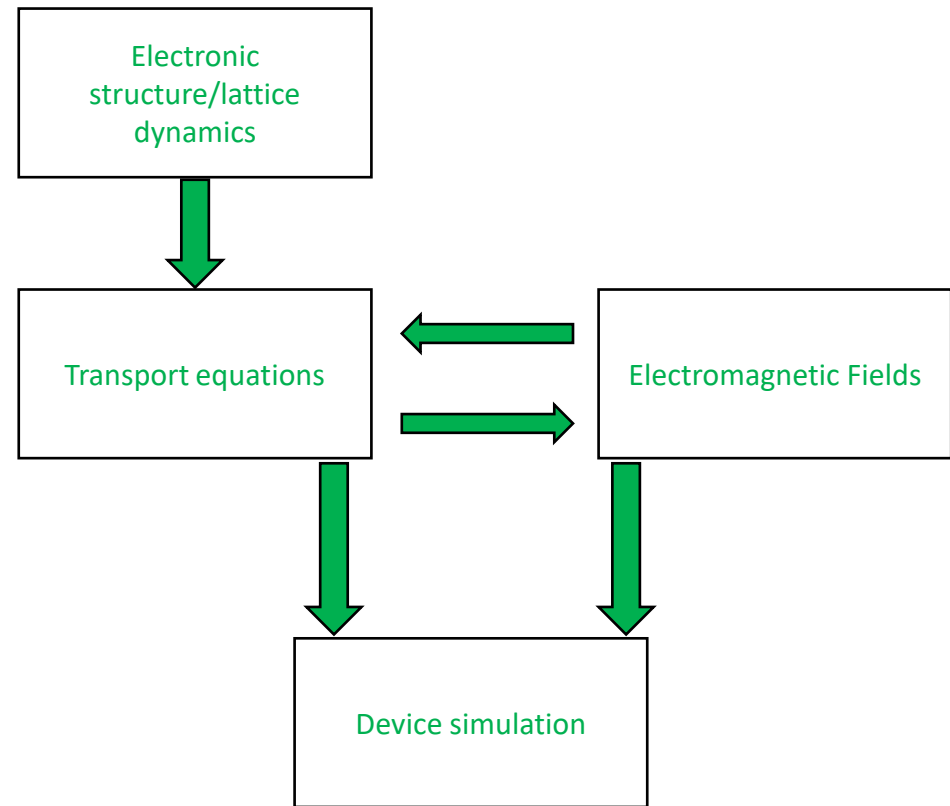
- Reasons why TCAD simulations are needed:
 - Market demands cycle of design to production of 18 months or less. Typically 2-3 months required for wafer tape out implies short time for development
 - Reduce cost to run experiments on new devices and circuits



Shrinking product life cycles in semiconductor industry over time

Introduction

- Main components of semiconductor device simulation include description of electronic structure, driving forces and transport phenomena
- The two kernels of semiconductor transport equations and fields that drive charge flow are coupled to each other and needs solving self-consistently



Transport regimes

- Usually only the quasi-static electric fields from the solution of Poisson's equation are necessary for EM solutions
- Transport regime in semiconductors depends on length scale

Modern Silicon technology already requires tools to describe transport in quantum regime

[D. K. Ferry and S. M. Goodnick, Transport in Nanostructures, 1997]

	$L \ll l_{e-ph}$			$L \sim l_{e-ph}$	$L \gg l_{e-ph}$
	$L < \lambda$	$L < l_{e-e}$	$L \gg l_{e-e}$		
Transport regime	Quantum	Ballistic	Fluid	Fluid	Diffusive
Scattering	Rare	Rare	$e-e$ (Many), $e-ph$ (Few)		Many
Model:					
Drift-diffusion					
Hydrodynamic		Quantum hydrodynamic			
Monte Carlo					
Schrödinger equation					
Green's function					
Applications	Nanowires, superlattices	Ballistic transistor	Present time ICs	Present time ICs	Older ICs

L : device length

l_{e-e} : electron-electron scattering length

l_{e-ph} : electron-phonon scattering length

λ : electron wavelength

Transport regimes

- Charge carrier dynamics in Si detectors usually does not require QM
- Semiclassical laws of motions apply
- Drift-diffusion equations are valid, provided the electron gas is in thermal equilibrium with lattice temperature ($T_n = T_L$)

$$R \sim \frac{h}{2\pi \langle I \rangle} \gamma v \sim 1.2 \text{ [nm]} \text{ Ionization radius for MIP in Si (Segre', Nuclei and Particles, Vol. II)}$$

$$n = \frac{dE}{dx} \rho \frac{L}{E_{th}} \frac{1}{\pi R^2 L} \sim 2 \cdot 10^{19} \text{ charge density within Ionization radius and } n^{-1/3} \sim 3.6 \text{ [nm]}$$

$$\lambda \leq \frac{h}{\sqrt{2meV_b}} \sim \begin{cases} 0.38 \text{ [nm]} @ 10 \text{ V} \\ 0.12 \text{ [nm]} @ 100 \text{ V} \end{cases} \text{ De Broglie wavelength of carriers @ full depletion}$$

Drift diffusion model

- The semiconductor equations derived from 1st moment of BTE are referred to as Drift Diffusion model
- The model consists of Poisson's equation, continuity and current density equations for electrons and holes
- They express charge and momentum conservation
- Their self-consistent solutions are obtained via discretization, using finite element methods (FEM)

$$\partial_t f + \mathbf{u} \cdot \nabla_{\mathbf{r}} f + \frac{\mathbf{F}}{\hbar} \cdot \nabla_{\mathbf{k}} f = C[f] \quad \text{BTE}$$

$$\text{div}(\varepsilon \cdot \text{grad} \psi) = q \cdot (n - p + N_A - N_D) \quad \text{Poisson}$$

$$\text{div} \mathbf{J}_n - q \cdot \frac{\partial n}{\partial t} = q \cdot R \quad \text{Continuity}$$

$$\text{div} \mathbf{J}_p + q \cdot \frac{\partial p}{\partial t} = -q \cdot R$$

$$\mathbf{J}_n = q \cdot n \cdot \mu_n \cdot \mathbf{E} + q \cdot D_n \cdot \text{grad} n$$

Current density

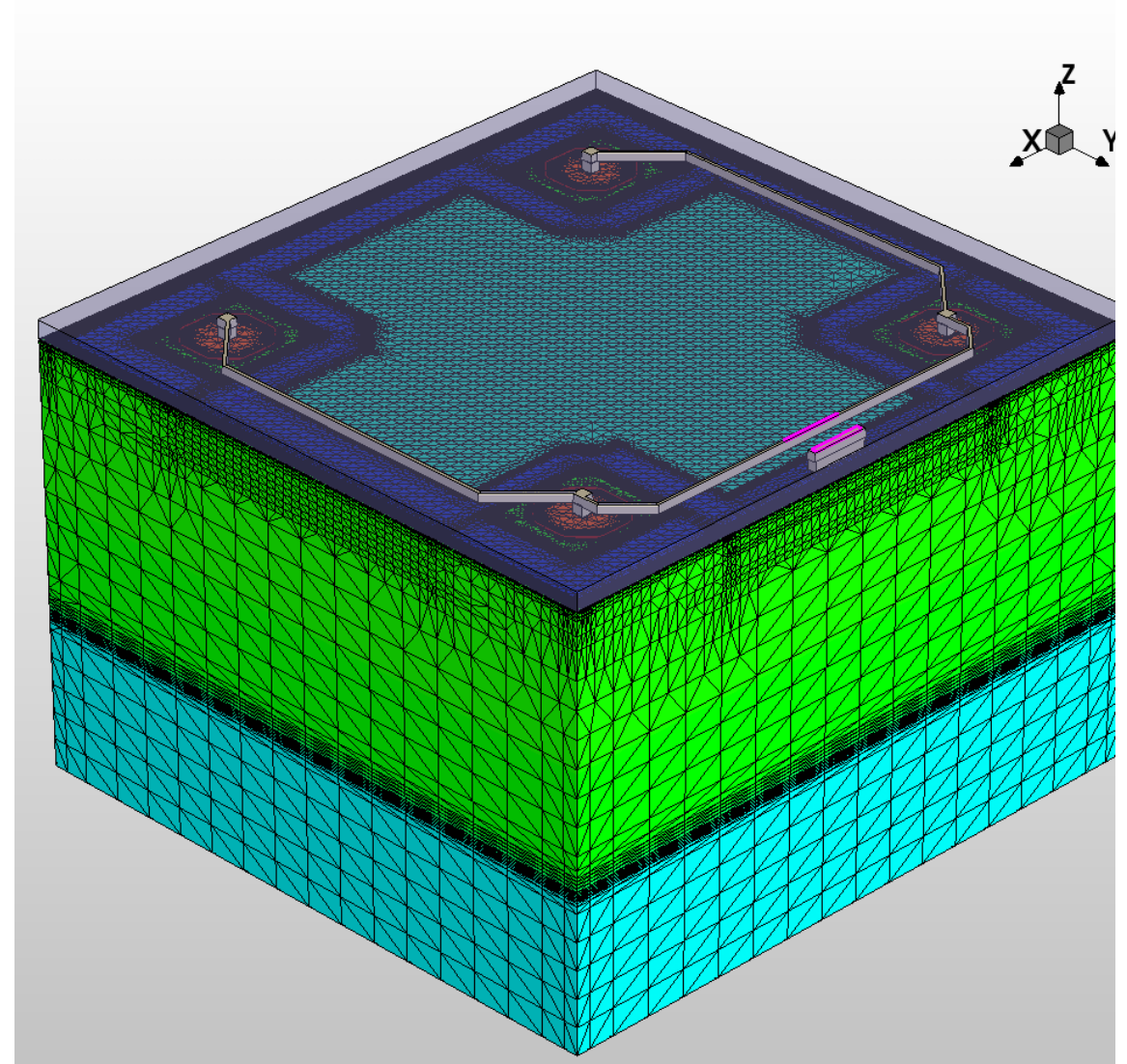
$$\mathbf{J}_p = q \cdot p \cdot \mu_p \cdot \mathbf{E} - q \cdot D_p \cdot \text{grad} p$$

Discretization and meshing

- The device simulations process consists of two steps:

1: The test volume is obtained through grid generation ('mesh generation')

2: Solve the discretized differential equations using Finite-Boxes method (box integration method) . This method integrates PDEs over the test volume.



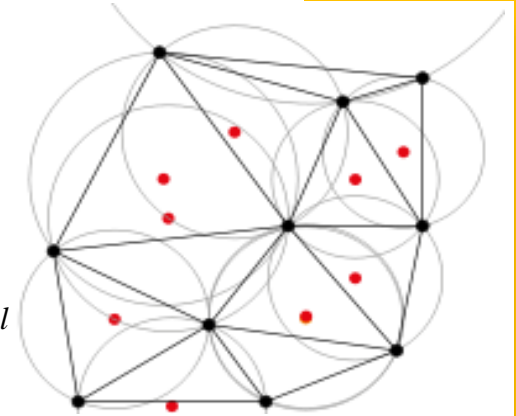
Discretization and meshing

- The meshing used in most finite elements methods (FEM) relies on Delaunay triangulations:

the interior of the circumsphere of each element contains no mesh vertices.

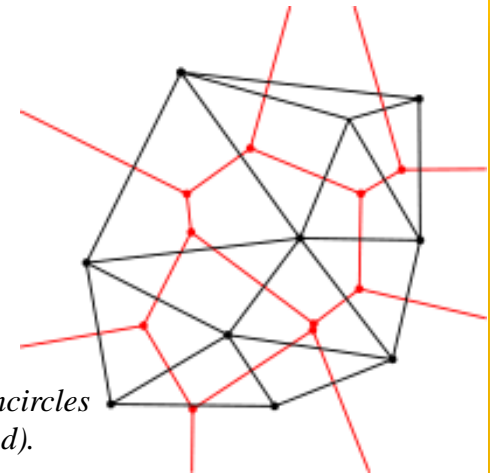
- The Delaunay triangulation of a discrete point set \mathbf{P} in general corresponds to the dual graph of the Voronoi diagram for \mathbf{P}

the set of all locations x closest to P_i than to any other point of the grid



The Delaunay triangulation with all the circumcircles and their centres

$$T_{D,k}(\mathcal{P}_{D,k}) \iff \exists \mathbf{x} \\ \mathbf{x} \in \Omega \quad \wedge \\ |\mathbf{x} - \mathbf{x}_i| = |\mathbf{x} - \mathbf{x}_j| \quad \forall P_i, P_j \in \mathcal{P}_{D,k} \quad \wedge \\ |\mathbf{x} - \mathbf{x}_i| < |\mathbf{x} - \mathbf{x}_k| \quad \forall P_i \in \mathcal{P}_{D,k}, P_j \notin \mathcal{P}_{D,k}$$



Connecting the centres of the circumcircles produces the Voronoi diagram (in red).

$$\Omega_i = \{ \mathbf{x} \mid |\mathbf{x} - \mathbf{x}_i| \leq |\mathbf{x} - \mathbf{x}_j| \quad \forall i \neq j, \mathbf{x} \in \Omega \}$$

Discretization and meshing

- Correct Delaunay triangulation guarantees element-volume conservation, important in many problems (diffusion, charge generation, et cetera)
- Delaunay triangulation maximizes the minimum angle.

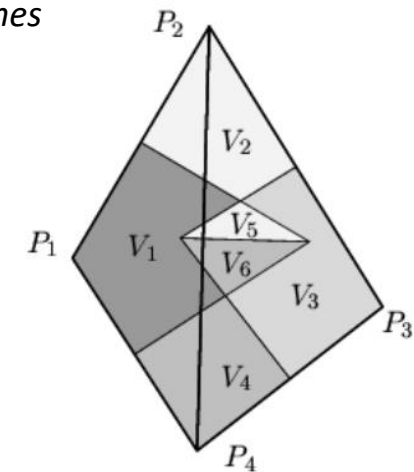
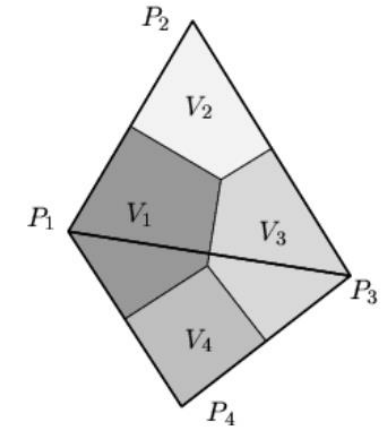
Voronoi boxes do not overlap (each circumcircle does not include a point of another triangle). Each can be uniquely assigned to its corresponding grid points.

$$P_i = V_i$$

Voronoi boxes do overlap (each circumcircle does include a point of another triangle). Each cannot be uniquely assigned to its corresponding grid points. Wrong volumes calculated

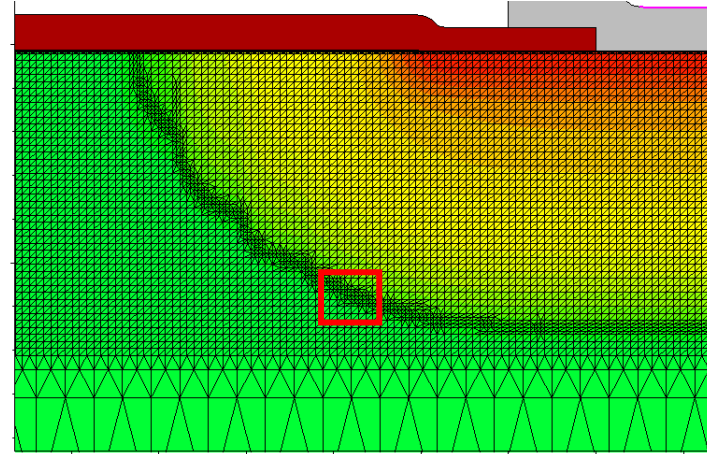
$$P_1 = V_1 + V_5 + V_6$$

$$P_3 = V_3 + V_5 + V_6$$



Discretization and meshing

- Discretization of equations imposes some constraints on spatial and temporal mesh size
- Mesh size should be smaller than Debye length (i.e. the characteristic length for screening of field by charges) where charge variations in space have to be resolved



$$L_D = \sqrt{\frac{\epsilon_s k_B T}{e^2 N}} \text{ Debye length}$$

$$N = 10^{13} [cm^{-3}]: L_D \approx 1.3 [um] @ T = 300 [K]$$

$$N = 10^{17} [cm^{-3}]: L_D \approx 13 [nm] @ T = 300 [K]$$

$$N = 10^{19} [cm^{-3}]: L_D \approx 1.3 [nm] @ T = 300 [K]$$

Discretization and meshing

- Also temporal ‘mesh’ size should be smaller than the dielectric relaxation time t_{dr} (i.e. time it takes to charge fluctuations to decay under the field they produce)
- Time interval Δt bigger than t_{dr} might give unrealistic transient results (‘oscillations’ in estimated transient currents)

$$\tau_{dr} \sim \frac{\epsilon_s}{eN\mu} \text{ Dielectric relaxation time}$$

$$N = 10^{13} [cm^{-3}], \mu_n \approx 1400 [cm^{-3}V^{-1}s^{-1}] @ T = 300 [K]: \tau_{dr} \approx 400 [ps]$$

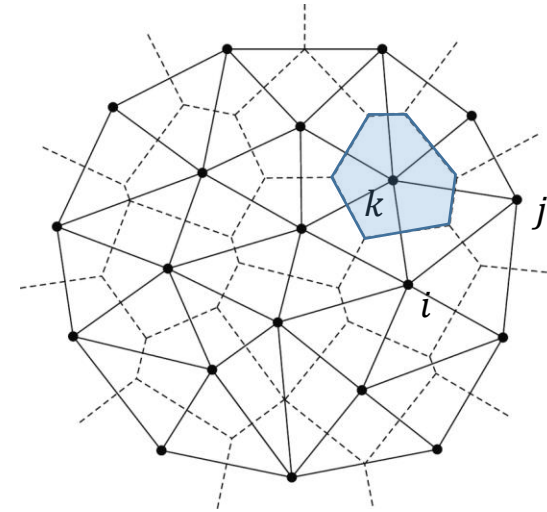
$$N = 10^{15} [cm^{-3}], \mu_n \approx 1350 [cm^{-3}V^{-1}s^{-1}] @ T = 300 [K]: \tau_{dr} \approx 4.8 [ps]$$

$$\frac{\partial \Delta n}{\partial t} = \frac{\Delta n(t=0)}{t_{dr}}$$

$$\Delta n(\Delta t) = \Delta n(0) - \Delta t \frac{\Delta n(0)}{t_{dr}}$$

Box integration method

- Discretization of Poisson's and continuity equations is done via Box Integration method
- The LHS of equations is transformed via Gauss' theorem and integrated over a Voronoi box Ω_k of point P_k



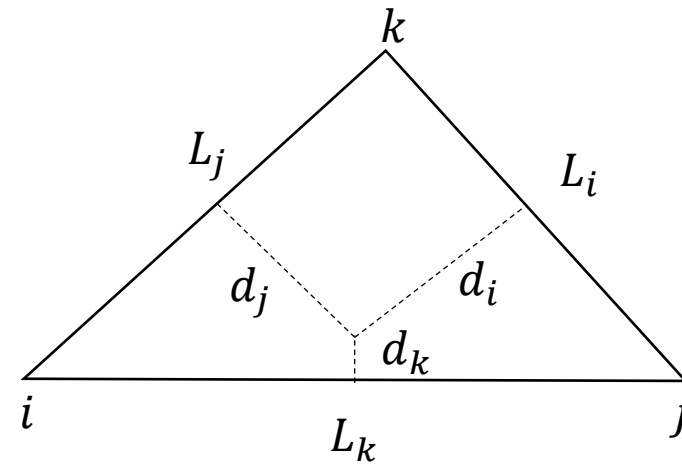
$$\operatorname{div}(\varepsilon \cdot \operatorname{grad} \psi) = q \cdot (n - p + N_A - N_D) \equiv \int D \cdot dS = \int \rho dV$$

$$\operatorname{div} \mathbf{J}_n - q \cdot \frac{\partial n}{\partial t} = q \cdot R$$

$$\operatorname{div} \mathbf{J}_p + q \cdot \frac{\partial p}{\partial t} = -q \cdot R$$

Box integration method

- Example of Poisson's discretization
- Assume that the electric potential is linearly varying over each elementary domain



i, j, k : nodal indices

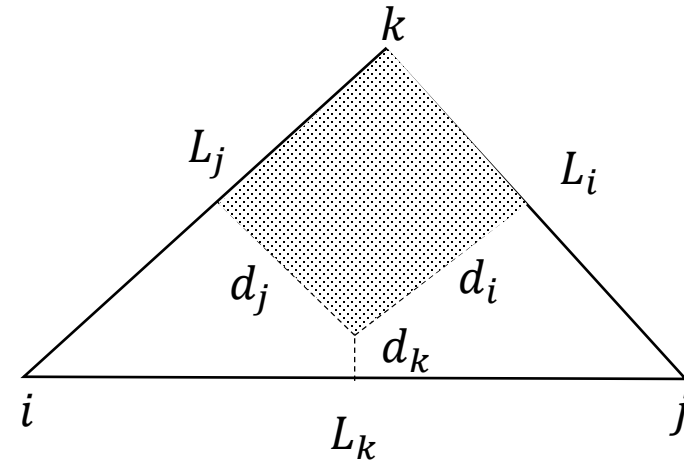
L_i, L_j, L_k : side vectors

L_i, L_j, L_k : magnitude side vectors

$$u := \frac{e}{k_B T} \varphi: \text{normalized potential}$$

Box integration method

- Components of D vector along sides $L_{i,j,k}$
- Flux of D vector associated to node k:
- Discretization of RHS is obtained by multiplying the node value of charge by the area of the portion of the Voronoi box

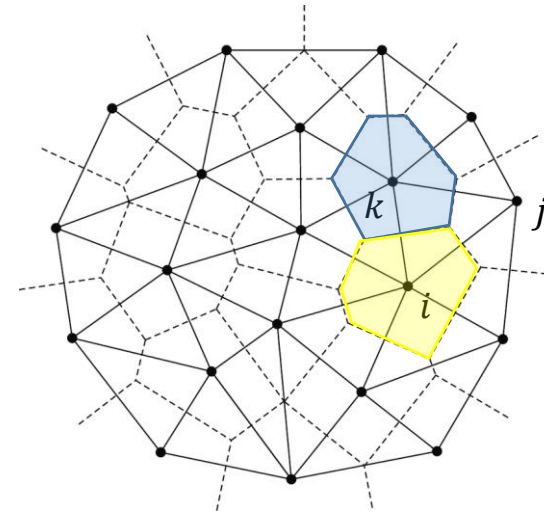


$$\frac{k_B T}{e} \epsilon_s \frac{1}{L_i} (u_j - u_k)$$
$$\frac{k_B T}{e} \epsilon_s \frac{1}{L_j} (u_k - u_i)$$
$$\frac{k_B T}{e} \epsilon_s \frac{1}{L_k} (u_i - u_j)$$

$$\frac{k_B T}{e} \epsilon_s \left[\frac{d_i}{L_i} (u_j - u_k) + \frac{d_j}{L_j} (u_i - u_k) \right] \text{ Flux of } D$$

Box integration method

- Summing over all points P_k of Voronoi boxes
- Same approach to discretize continuity equations for electrons and holes



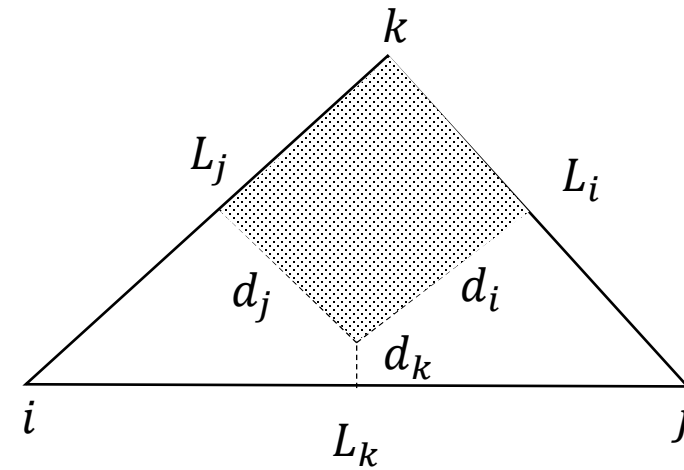
$$\sum_k D_{ik} A_{ik} = \rho_k V_k \quad \begin{array}{l} A_{ik}: \text{area of } K - V_{\text{box}} \\ D_{ik}: \text{projection along grid line} \end{array}$$

$$\sum_k J_{n,ik} A_{ik} = e \left(R_k + \frac{d}{dt} n_k \right) V_k$$

$$\sum_k J_{p,ik} A_{ik} = e \left(R_k + \frac{d}{dt} p_k \right) V_k$$

Scharfetter-Gummel discretization

- In case of no strong generation-recombination current density varies little within each domain
- Still this implies an exponential dependence of electron / hole density with position along grid's edge
- Using previous discretization method would require very dense mesh: Scharfetter-Gummel technique includes such dependence, requiring less grid points [D. L. Scharfetter and H. K. Gummel, "Large-signal analysis of a silicon read diode oscillator," IEEE Trans. Electron Devices, vol. ED-16, pp. 64–77, Jan. 1969].



$$\mathbf{J}_n = q \cdot n \cdot \mu_n \cdot \mathbf{E} + q \cdot D_n \cdot \text{grad } n$$

$$\mathbf{J}_p = q \cdot p \cdot \mu_p \cdot \mathbf{E} - q \cdot D_p \cdot \text{grad } p$$

$$u := \frac{e}{k_B T} \varphi$$

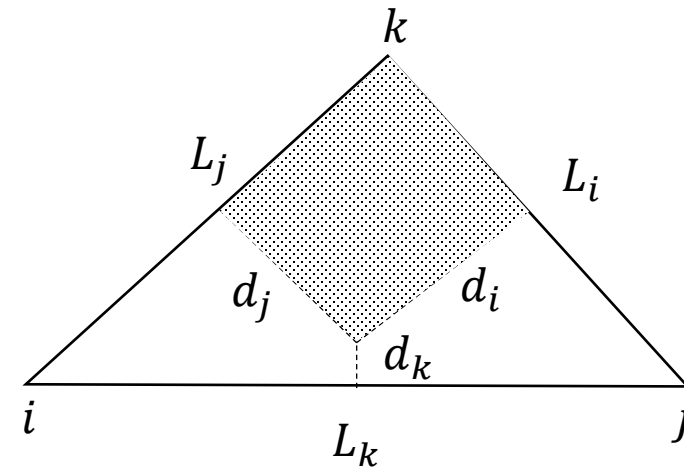
$$D_n := \frac{k_B T}{e} \mu_n$$

$$J_n := e D_n [\nabla n - n \nabla u] \quad \text{from } J_n$$

$$J_{nk} := e D_n \left[\frac{dn}{dl_k} - n \frac{du}{dl_k} \right] \quad \text{projection along } L_k \sim \text{constant}$$

Scharfetter-Gummel discretization

- Assume u varies linearly along the edge and current density \simeq constant over the domain
- Define reduced current and assume and average diffusion along the edge
- Obtain first order equation in n along the edge



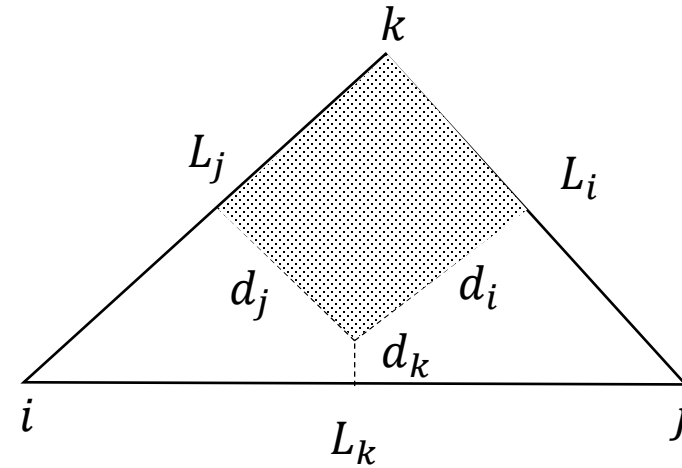
$$u = \frac{u_j - u_i}{L_k} l_k + u_i = a_k l_k + u_i$$

$$j_{nk} := \frac{J_{nk}}{eD_{nk}}, \quad D_{nk} := \langle D_{ni}, D_{nj} \rangle$$

$$j_{nk} = \frac{dn}{dl_k} - na_k$$

Scharfetter-Gummel discretization

- Integrate from node i to node j, i.e. for $l_k=[0, L_k]$
- Obtain expression relating potential and carriers concentration



$$\int_0^{L_k} \exp(-a_k l_k) j_{nk} = \int_0^{L_k} \exp(-a_k l_k) \left(\frac{dn}{dl_k} - n a_k \right) dl_k$$

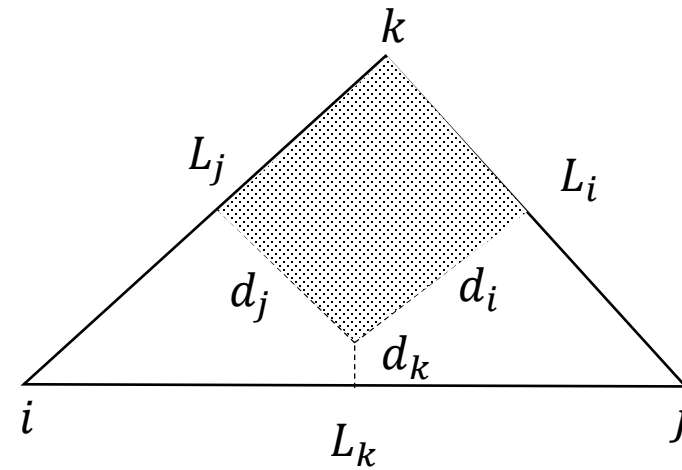
$$= \int_0^{L_k} \frac{d}{dl_k} (\exp(-a_k l_k) n) dl_k$$

$$j_{nk} \frac{1}{a_k} (1 - \exp(-u_{ji})) = \exp(-u_{ji}) n_j - n_i \quad , u_{ji} = u_j - u_i$$

$$j_{nk} = a_k \left(\frac{n_j}{\exp(u_{ji}) - 1} + \frac{n_i}{\exp(-u_{ji}) - 1} \right)$$

Scharfetter-Gummel discretization

- Obtain the flux of current density relative to node k
- Scharfetter –Gummel discretization requires less fine mesh as the exponential dependence of carriers concentration is included in the discretization scheme
- It also depends on boundary values, i.e. 2D and 3D cases can be reduced to local 1D cases



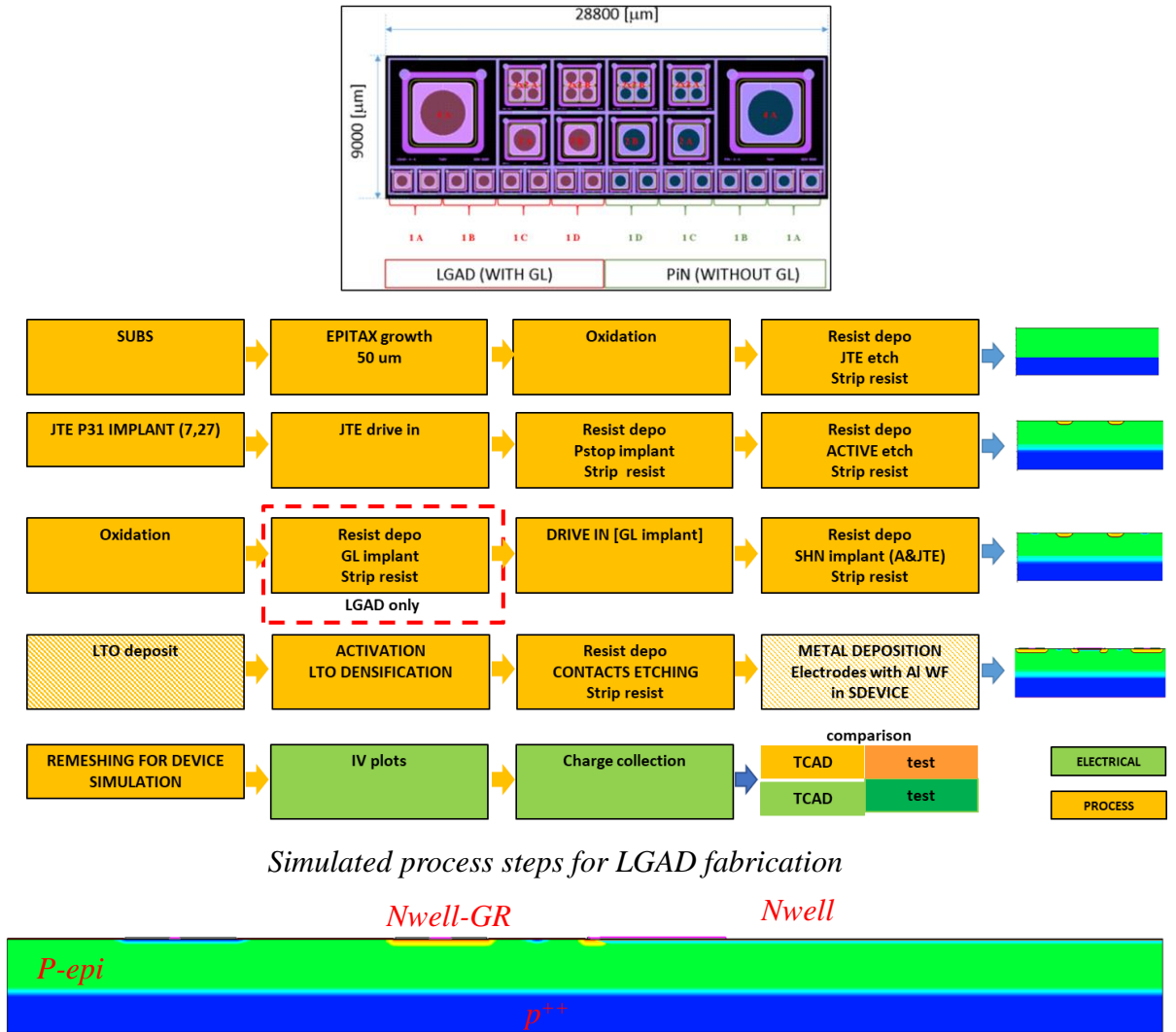
$$j_{nk} = \frac{1}{L_k} \left(\frac{u_{ji}n_j}{\exp(u_{ji})-1} - \frac{u_{ij}n_i}{\exp(u_{ij})-1} \right)$$

$$j_{nk} = \frac{1}{L_k} (B(u_{ji})n_j - B(u_{ij})n_i) \quad \text{Bernoulli function } B(x) := \frac{x}{\exp(x) - 1}$$

$$\begin{aligned} \nabla \cdot J_{nk} &= eD_{ni} \frac{d_i}{L_i} (B(u_{jk})n_j - B(u_{kj})n_k) + eD_{ni} \frac{d_j}{L_j} (B(u_{ik})n_i \\ &\quad - B(u_{ki})n_k) \end{aligned}$$

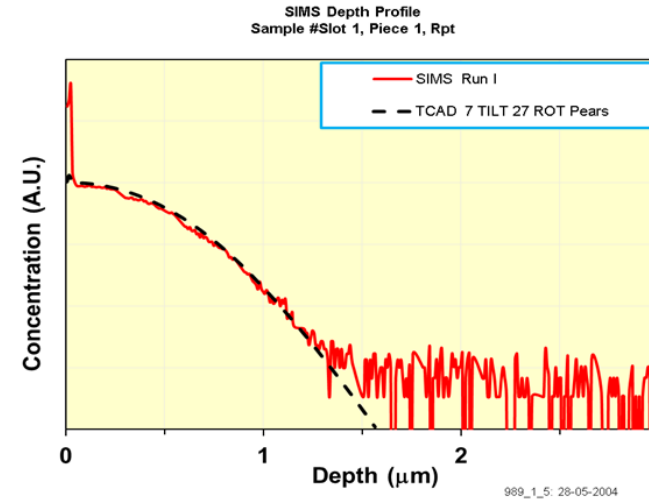
Simulation examples

- Examples from Synopsys TCAD (more on this from N. Owen lectures)
- Beside electrical simulations, simulation of processes of device fabrication is possible
- Most of the typical fabrication process steps can be simulated

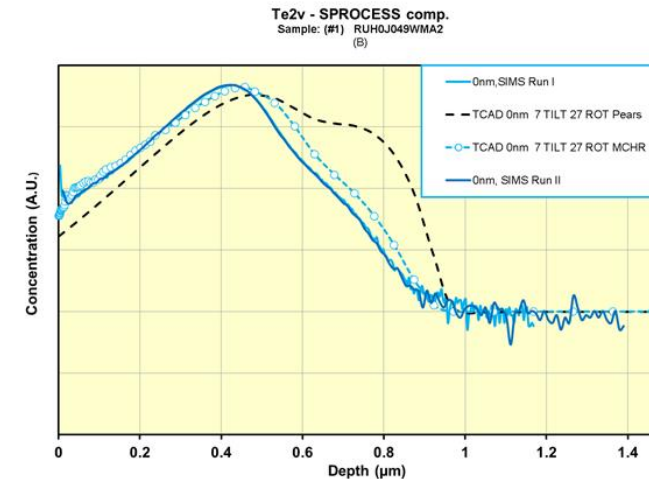


Simulation examples

- High energy implants of ions can be simulated, either analytically or via MC
- Creation of defects following implantation can be simulated



SIMS and Pearson IV distribution – 31P

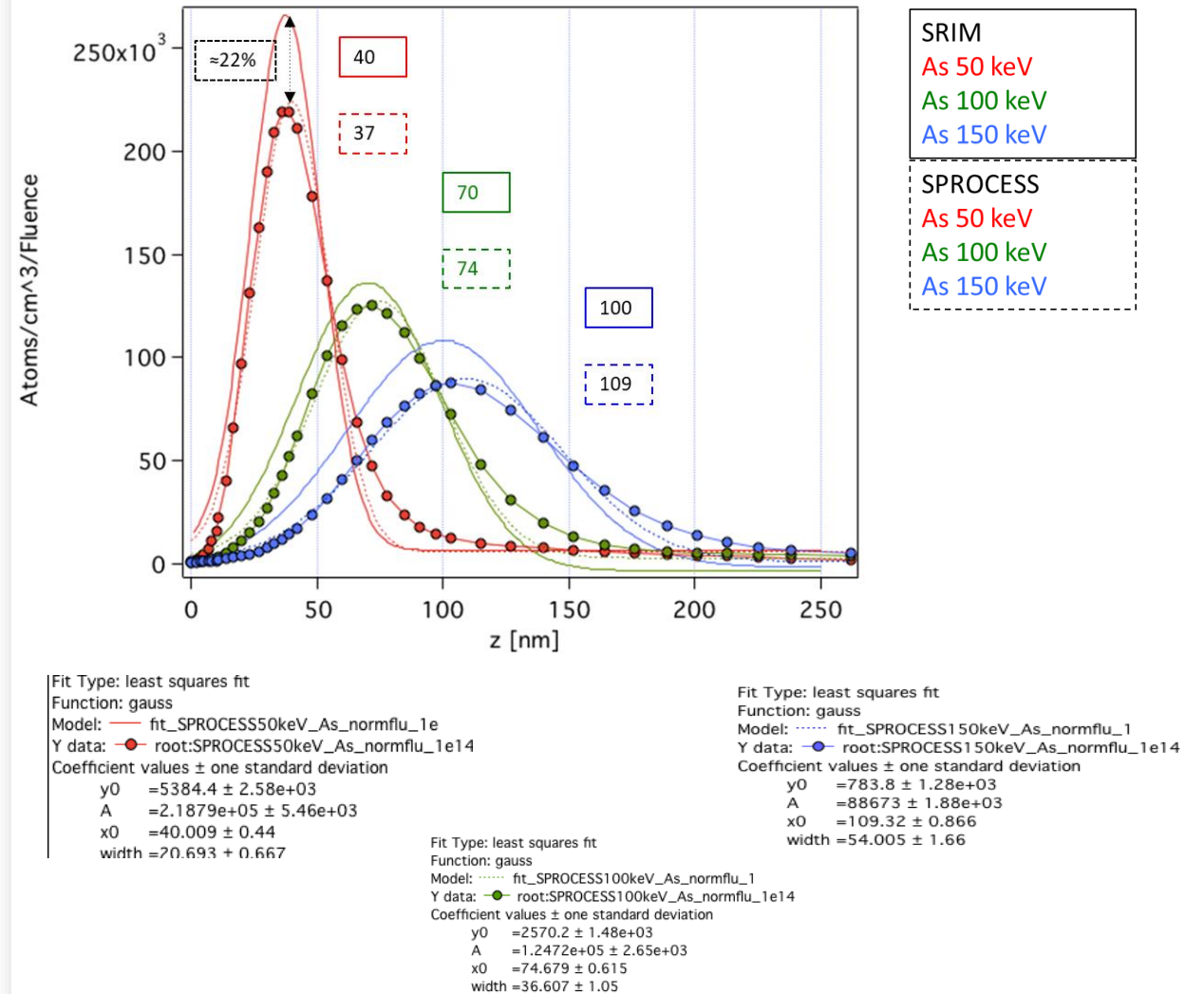


SIMS, Pearson IV distribution and MC run – 11B

Simulation examples

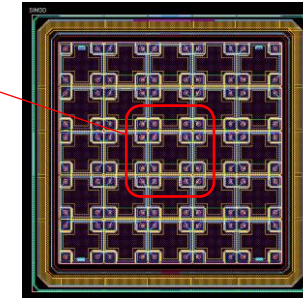
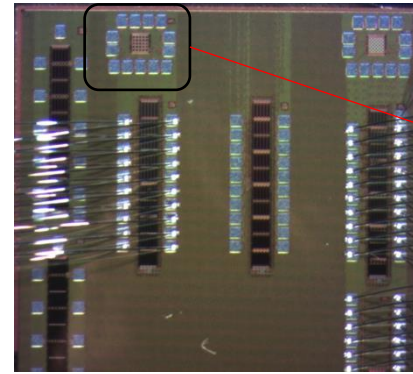
- At least with As, MC (SRIM) and SPROCESS predictions on doping seem to agree within $\approx 20\%$
- Note: SRIM assumes amorphous Si, $\langle 100 \rangle$ used for SPROCESS, but 1D

SRIM (Stopping and Range of Ions in Matter, <http://www.srim.org/>)

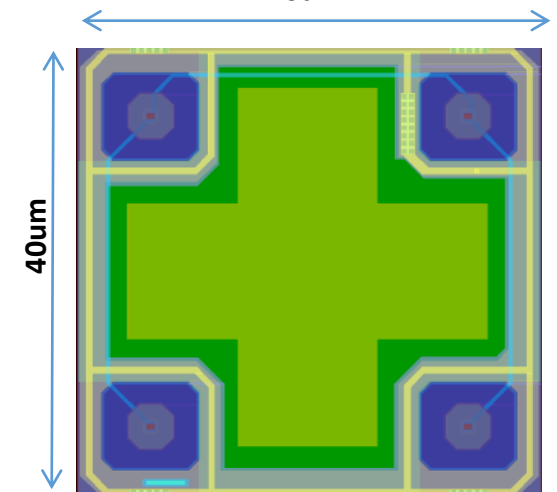
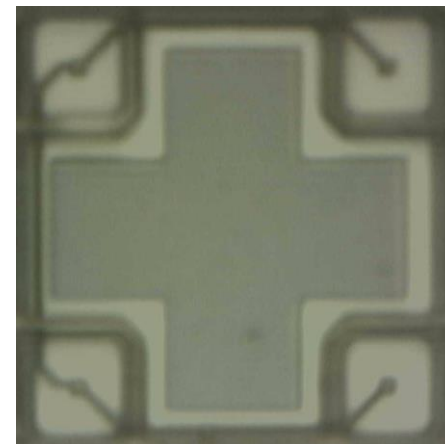


Simulation examples

- Electrical simulation of a CMOS sensors (OVERMOS)
- A TCAD model of fabrication process of OVERMOS has been developed to investigate and predict the performances of the sensor



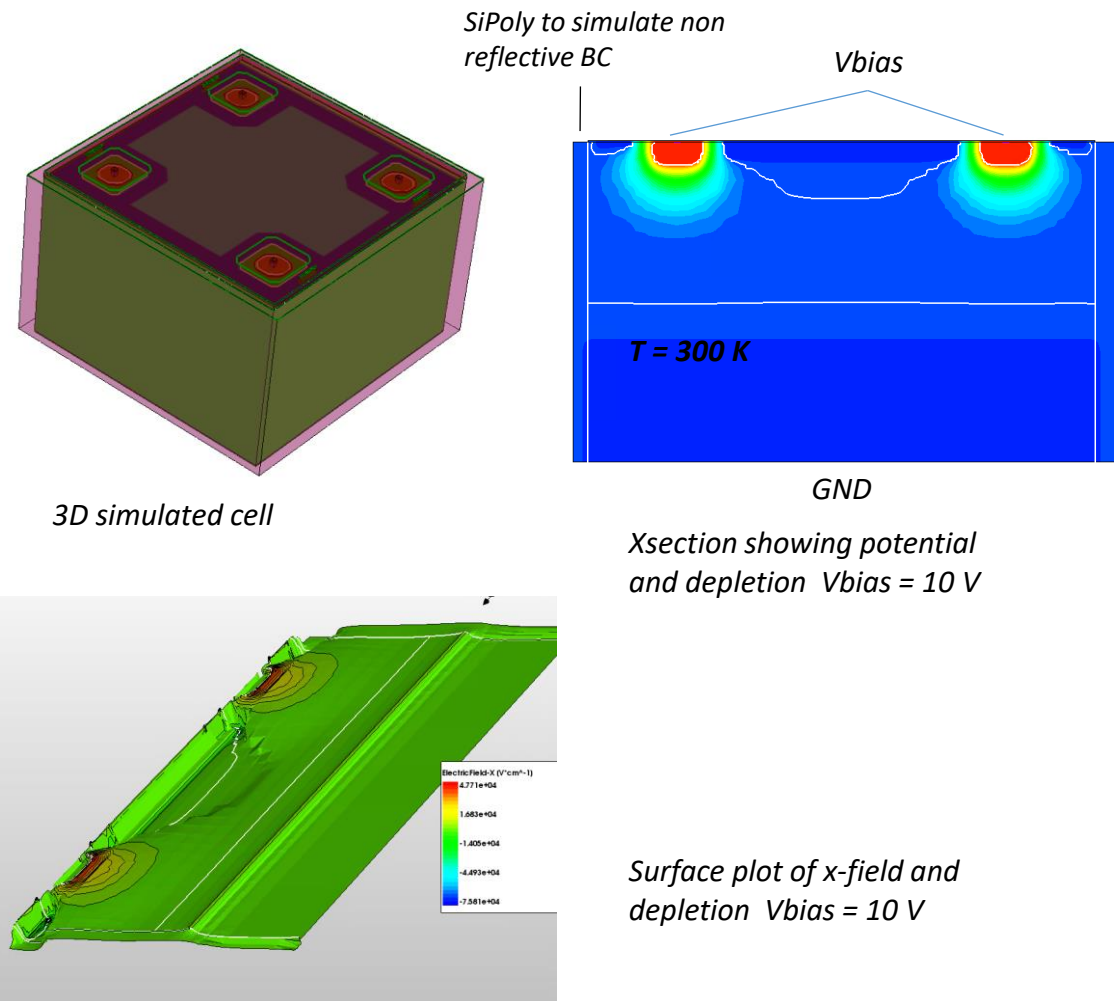
Photograph of OVERMOS test structure and simulated cell
40um



Photograph of OVERMOS cell and .gds layout

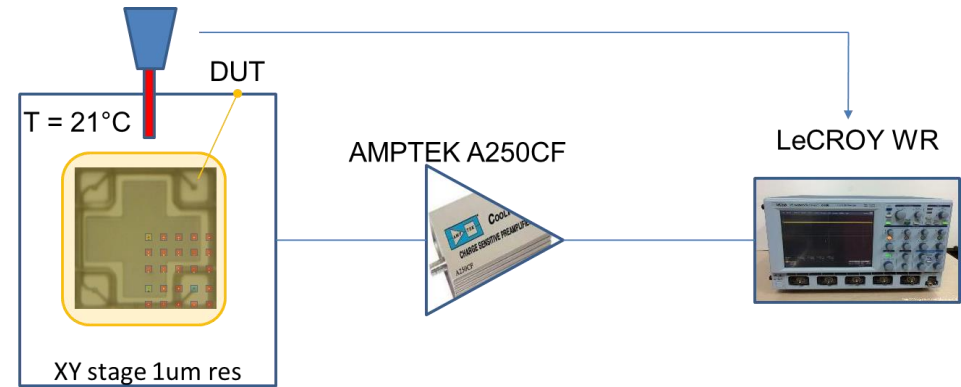
Simulation examples

- Internal field configuration vs. bias and temperature
- DC and AC characteristics can be obtained from the simulated model

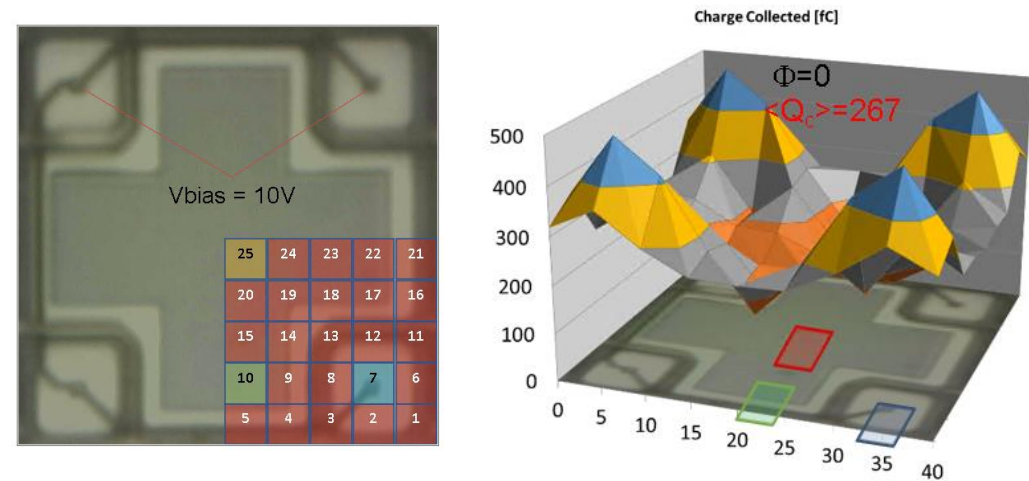


Simulation examples

- Charge collection is simulated using laser light injection and compared with test results
- Laser beam is $5 \times 5 \mu\text{m}^2$ around 4.5 ns pulse width, 1064 nm wavelength, $\sim 10 \text{ pJ}$
- These values are introduced in the simulator



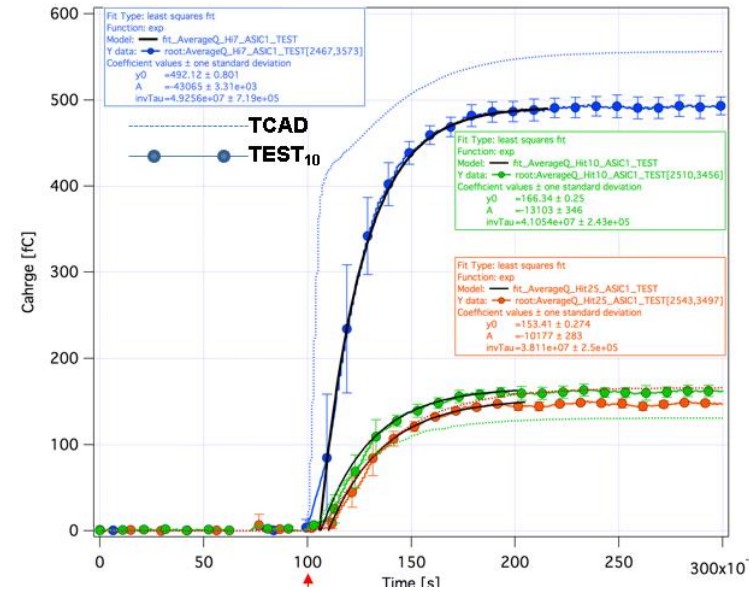
Test setup for charge collection measurement



Charge is injected via laser at three different locations on cell. Results are mirrored to obtain a map of collected charge vs. position

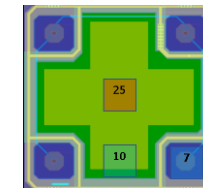
Simulation examples

- Effects of SiO₂ reflection and attenuation of IR light can be implemented
- Quantum yield of optical generation, polarization, tilting, pulse width et cetera can all be included in the simulation
- TCAD simulations of non-irradiated OVERMOS reproduce experimental results, both in DC and in CC, with maximum discrepancy of the order of ~20%



Transient of charge collection measurement and simulation

Q _{coll}	Test	TCAD	Δ%
<Qh7>	492	556	-13
<Qh10>	166	131	21
<Qh25>	153	166	-8.4



Thank you

giulio.villani@stfc.ac.uk

- Introduction to simulation
- Needs and transport regimes
- Meshing and discretization. Intro to DD model discretization. SG method
- Some examples of TCAD simulations: process and electrical device simulations, charge collection